J IRAN CHEM SOC
DOI 10.1007/s13738-017-1157-2

ORIGINAL PAPER

Magnetic nanoparticles grafted L-carnosine dipeptide: remarkable catalytic activity in water at room temperature

Farhad Panahi[1,2] · Foroogh Bahrami[1] · Ali Khalafi-Nezhad[1]

Received: 27 March 2017 / Accepted: 12 June 2017

Abstract Modification of magnetic nanoparticle surface with L-carnosine dipeptide was developed using a simple chemical process. In order to synthesize this catalyst system, first, magnetic nanoparticles were modified with vinyl groups using trimethoxy(vinyl)silane. Next, the vinyl groups were oxidized with H_2O_2 to give the epoxy-functionalized MNPs. Reaction of L-carnosine with epoxide rings via amino group resulted in the functionalization of MNPs surface with L-carnosine, covalently. To explore high catalytic activity of this material, L-carnosine grafted on magnetic nanoparticles (Fe_3O_4@SiO_2@LCar; L-CarMNP) was used as a highly efficient heterogeneous nano-organocatalyst in a multicomponent reaction in aqueous medium at room temperature. It was reusable at least for eight times without a significant decrease in its catalytic activity. The catalytic activity of L-CarMNP was compared with other magnetic nano-organocatalyst, and results demonstrate that L-CarMNP has high catalytic activity related to others tested.

Keywords Magnetic nanoparticles · L-carnosine · Dipeptide · Heterogeneous catalyst · Organocatalyst · Water

Introduction

Organocatalysis is of significant relevance for contemporary organic chemistry, playing a key role in organic synthesis [1–3]. Different small molecules have been introduced as organocatalyst to be used in many organic reactions [4–9]. Amino acids and peptides are an important class of organic molecules which have been widely used in organic synthesis as organocatalyst or ligand in transition metal catalysis [10–16]. Due to many advantages, amino acid and peptide organocatalysts are able to be used as heterogeneous and thus required a solid support of metal oxides or polymers which both of them are established to be suitable for this purpose [17–24]. Although a number of heterogeneous organocatalysts based on amino acid have been synthesized, catalysis under aqueous conditions is desirable for various reasons, particularly due to the fact that amino acids have high solubility in water and so offer high activity [15]. This feature also avoids the unfavorable organic wastes, which readily occurs under organic solvent conditions, reducing the environmental friendly of the catalysis process [25, 26]. In the presence of heterogeneous catalysts and in aqueous environments, the solubility of reactants represents challenges in reserve efficiency, exacting because of low interaction of catalyst and substrates [27, 28]. On the other hand, magnetic nanoparticles (MNPs) have diverse "solubilities" in aqueous and non-aqueous solvents, depending on their size and the type of modifying organic moiety. The ability to be soluble or dispersed (for short or long periods) and the constancy of MNPs in

Electronic supplementary material The online version of this article (doi:10.1007/s13738-017-1157-2) contains supplementary material, which is available to authorized users.

✉ Farhad Panahi
fpanahi@aut.ac.ir

✉ Ali Khalafi-Nezhad
khalafi@susc.ac.ir

[1] Department of Chemistry, College of Sciences, Shiraz University, Shiraz 71454, Iran

[2] Department of Polymer Engineering and Color Technology, Amirkabir University of Technology, Tehran, Iran

Published online: 20 June 2017

liquid phase are very important factors in catalysis applications [29–34]. In this way, extensive efforts have been made to attain a higher solubility of MNPs, especially in aqueous media [35]. Highly soluble MNPs-based catalysts have much greater catalyst activity in organic reactions and act same as pseudo-homogeneous catalysis. With increase in water well-matched organic moieties on the surface of MNPs, their water solubility is enhanced. Amino acids and peptides due to the polar organic functional groups have this capability to improve the water solubility of MNPs [36–39]. In other side, amino acids and peptides have remarkable catalyst activity in organic transformations. Thus, by functionalization of MNPs surface with amino acids and peptides it is possible to synthesize an efficient heterogeneous magnetic nano-organocatalyst to accomplish organic reactions in water. Previously, we reported an efficient strategy on modification of MNPs surface with organic moieties using the ring opening of generated oxiran rings on MNPs surface with nucleophile organic molecules [40–44]. This strategy opens up our hand to graft organic molecules on MNPs surface simply. In this study, the catalytic activities of three different types of heterogeneous magnetic nano-organocatalyst were evaluated in a multi-component reaction in aqueous media (Scheme 1).

The LPMNP [40] and L-CyMNP [41] catalysts were previously synthesized, characterized, and used in organic transformations. In this work, L-carnosine grafted on magnetic nanoparticles (L-CarMNP) was synthesized according to our previous strategy and introduced as an efficient heterogeneous organocatalyst in organic transformations [45].

Results and discussion

For synthesis of L-CarMNP, first, trimethoxy(vinyl)silane was tethered to the surface of iron oxide nanoparticles, and a subsequent epoxidation of the vinyl group with H_2O_2 gave the desired epoxy-functionalized MNPs. L-Carnosine has an amino group which can react with epoxide ring and open it, because it has nucleophilic power [46]. Ring opening of oxiran rings on the surface of MNPs with L-carnosine resulted in the production of Fe_3O_4@SiO_2@LCar (L-CarMNP) catalyst. The L-CarMNP catalyst was characterized using FTIR, SEM, XRD, and elemental analysis techniques. A comparison between the FTIR spectra of Fe_3O_4, Fe_3O_4@SiO_2, VMNP, L-carnosine, and L-CarMNP material was made, and results show the existence of L-carnosine moiety in the structure of magnetic nanoparticles (see ESI). In accordance with FTIR spectra, the peak at 1635 cm^{-1} is confirmed the presence of L-carnosine in the structure of L-CarMNP catalyst because this peak attributed to the C=O bond [45]. Also, distinguished peaks observed at 2923, 2314, 894, and 795 cm^{-1} establish the presence of L-carnosine moiety in the structure of synthesized catalyst [47]. The SEM image of the synthesized catalyst was recorded and is represented in Fig. 1. Considering the SEM image, it is clear that the L-CarMNPs are regular in shape and approved in an approximately good arranged mode. This image also established this point that the L-CarMNPs are created with near sphere-shaped morphology. According to the particle analyzer result, the average diameter of the synthesized L-CarMNPs based on the proposed procedure is estimated to be about 18–30 nm.

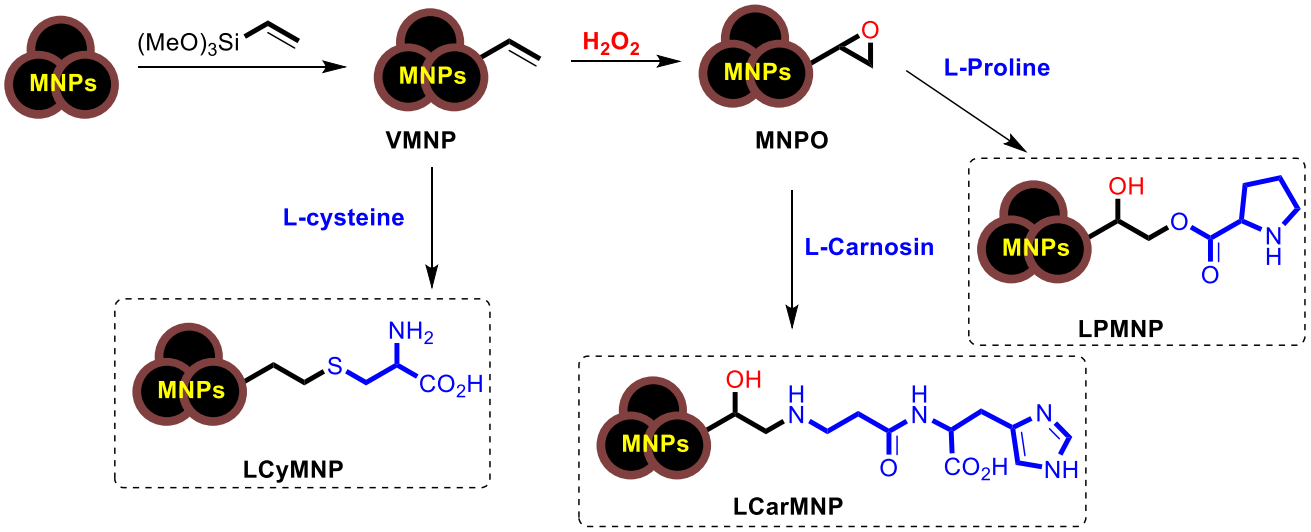

Scheme 1 The chemical structures of three different MNPs-supported organocatalyst

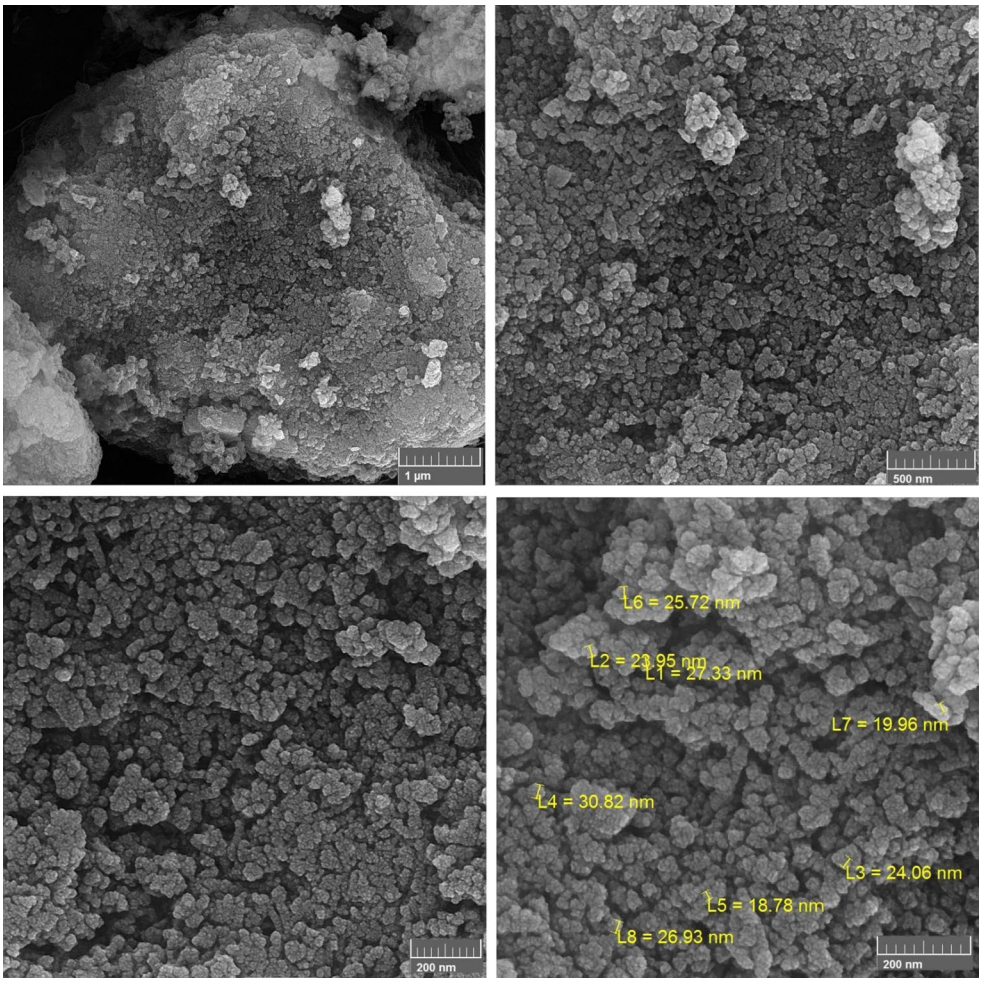

Fig. 1 The SEM images of L-CarMNP catalyst

The XRD pattern of the L-CarMNP catalyst also shows the magnetic nanoparticle nature of catalyst after modification (Fig. 2).

The peaks are indexed as the (220), (311), (400), (422), (511), (440), and (533) planes of the Fe_3O_4 nanoparticles (JCPDS no. 19-0629) [48]. The strongest peaks of the

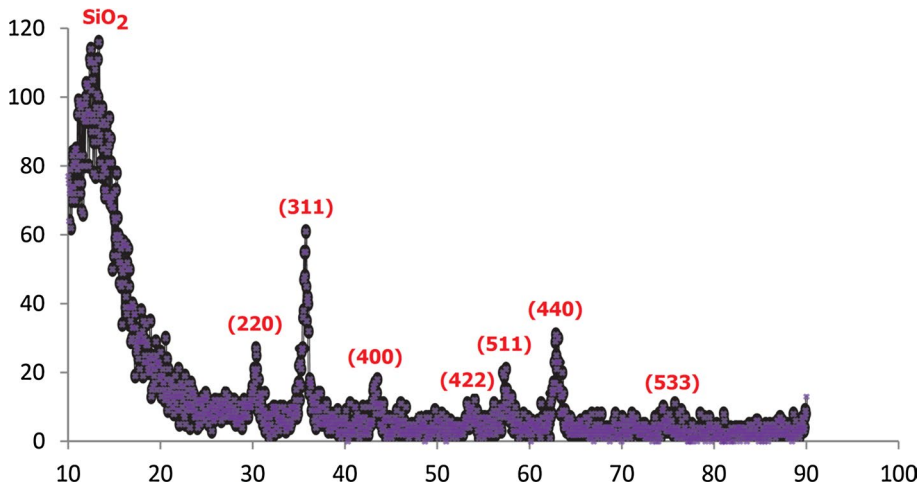

Fig. 2 The XRD pattern of L-CarMNP catalyst

XRD pattern correspond to SiO_2, demonstrating the core–shell structure of material. Also, the elemental analysis of the L-CarMNP material demonstrates the presence of C, N, and H which confirms the presence of L-carnosine on the surface of magnetic nanoparticles. According to the data obtained from elemental analysis, it is concluded that there is about 0.5 mmol of L-carnosine per 1 g of material using our procedure (catalyst loading is 0.5 mmol/g). The functional groups in the structure of L-CarMNP are carboxylic acid, amino group, hydroxy group, amide bond, and imidazole ring which can act as organocatalytic centers for promotion of an organic reaction [16]. In order to show the catalytic activity of L-CarMNP in organic reactions, it was used as a magnetic reusable organocatalyst in a multicomponent reaction (MCR). MCRs are known as an applicable strategy in organic synthesis for synthesis of complex molecules from simple starting materials [49–54]. The most important classes of organic molecules that can be synthesized using MCRs are acridine and xanthene derivatives. Acridine and xanthene derivatives have important biological activities such as fungicidal, antimicrobial, anti-parasitic, anti-inflammatory, anticancer, and anti-viral activities [55–58]. A reaction model was selected and the catalytic activity of the L-CyMNP, LPMNP, and L-CarMNP catalysts was evaluated (Table 1).

As given in Table 1, in the absence of catalyst no product was observed (entry 1). In the presence of Fe_3O_4@SiO_2 as catalyst, about 18% of product of **4a** was detected (Table 1, entry 2). Then, we applied the L-CarMNP material as catalyst for this reaction and 95% of product was obtained after 2 h (Table 1, entry 3). These results were suitable but were not satisfactory for us because we followed the accomplishment of reaction in water as green solvent at room temperature conditions. Thus, we checked reactions under these conditions, and interestingly, it was observed that in water solvent at room temperature after 6 h about 92% of product was produced. These results were very exciting for us, demonstrating remarkable catalytic activity of L-CarMNP. Different amounts of catalyst were checked in order to find optimized catalyst loading. It was observed that by increasing the amount of catalyst the yield of product remained unchanged and as result of reducing the amount of catalyst

Table 1 Optimization of reaction conditions for synthesis of acridines

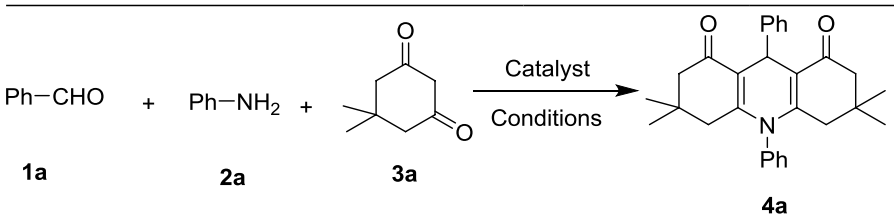

1a **2a** **3a** **4a**

Entry	Catalyst (mol %)	Solvent	T (°C)	Time (h)	Yield **4a** (%)[a]
1	None	EtOH	80	12	0
2	Fe_3O_4@SiO_2	EtOH	80	12	18[c]
3	L-CarMNP (5)	EtOH	80	2	95
4	L-CarMNP (5)	H_2O	80	2	93
5	L-CarMNP (5)	H_2O	rt	6	92
6	L-CarMNP (6)	H_2O	rt	6	93
7	L-CarMNP (4)	H_2O	rt	8	89
8	L-CarMNP (5)	CH_3CN	70	12	60
9	L-CarMNP (5)	$PhCH_3$	80	12	55
10	L-CarMNP (5)	DMF	100	12	80
11	L-CyMNP (5)	H_2O	rt	12	30
12	L-CyMNP (5)	H_2O	80	6	73
13	LPMNP (5)	H_2O	rt	12	20
14	LPMNP (5)	H_2O	80	5	75
15	L-carnosine	H_2O	rt	12	60
16	L-Proline	H_2O	rt	12	30
17	L-Cysteine	H_2O	rt	12	28

Reaction conditions: **1a** (1 mmol), **2a** (1 mmol), **3a** (2.2 mmol), and solvent (3 mL)

[a] Isolated yield

[b] 0.05 g of catalyst was used

Table 2 Synthesis of diverse xanthene and acridine derivatives using L-CarMNP under optimized conditions[a]

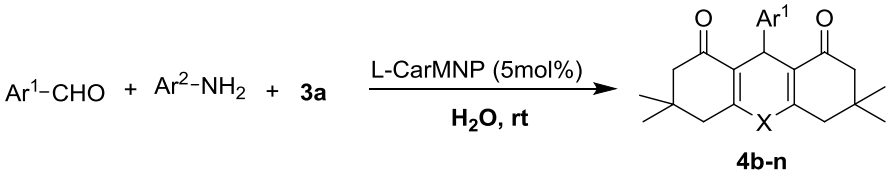

4b-n

Entry	Ar^1	X	Prod.	Time (h)	Yield (%)[b]
1	3-NO_2-Ph	4-F-Ph-N	**4b**	6	89
1	4-Cl-Ph	4-Cl-Ph-N	**4c**	6	92
2	4-NO_2-Ph	4-OMe-Ph-N	**4d**	5	94
3	4-Cl-Ph	4-OMe-Ph-N	**4e**	5	92
4	4-Cl-Ph	4-F-Ph-N	**4f**	6	90
5	4-NO_2-Ph	4-F-Ph-N	**4g**	6	91
6	4-OH-Ph	4-OMe-Ph-N	**4h**	8	89
7	4-NO_2-Ph	O	**4i**	6	90
8	4-Cl-Ph	O	**4j**	6	92
9	3-Cl-Ph	O	**4k**	8	88
10	4-F-Ph	O	**4l**	7	90
11	4-OH-Ph	O	**4m**	12	85
12	3-CH_3-Ph	O	**4n**	10	87

[a] Reaction conditions: aldehyde (1 mmol), amine (1 mmol), 3a (2.2 mmol), catalyst (5 mol %), and solvent (3 mL)

[b] Isolated yield

reduction in yield was observed (Table 1, entries 6, 7). The activity of L-CarMNP in other solvents was also tested, but a significant decreasing in reaction yield was observed (Table 1, entries 8–10).

A comparison between the catalytic activity of L-CarMNP and some other catalyst systems was made, and results demonstrating amazing catalytic activity of L-CarMNP related to other catalyst systems were investigated (Table 1, entries 11–17). For example, less than 30% of product was isolated using LPMNP [40] and L-CyMNP [41] catalysts at room temperature in water solvent. The reaction yields for these catalyst systems were in the range of 75% at higher temperate. Interestingly, L-carnosine in comparison with two other amino acids (L-cysteine and L-proline) has higher activity in water at room temperature. More importantly, the catalytic activity of L-carnosine is less than supported counterpart, demonstrating synergetic effect between MNPs support and L-carnosine. Furthermore, the separation of product from reaction mixture is difficult. These results also show that the connection of L-carnosine via NH group to the surface of magnetic nanoparticles improves its catalytic activity and applicability.

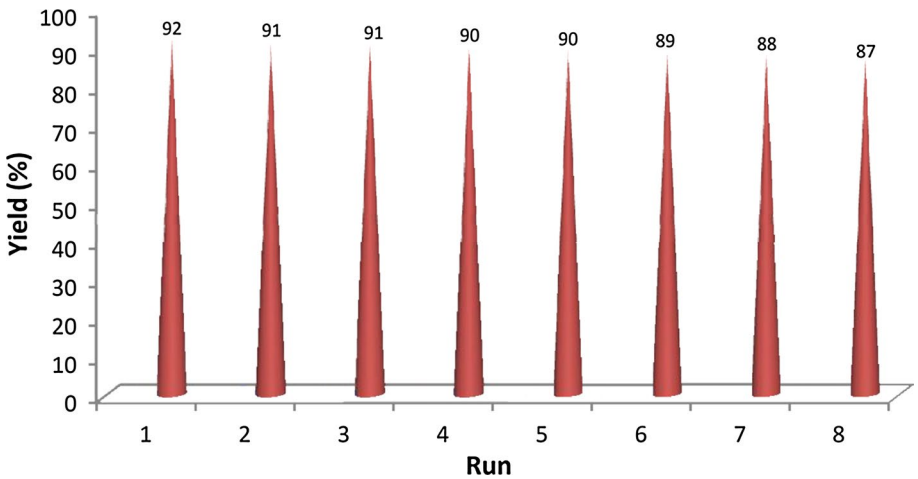

Fig. 3 Catalytic recovery times of L-CarMNP catalyst for eight runs

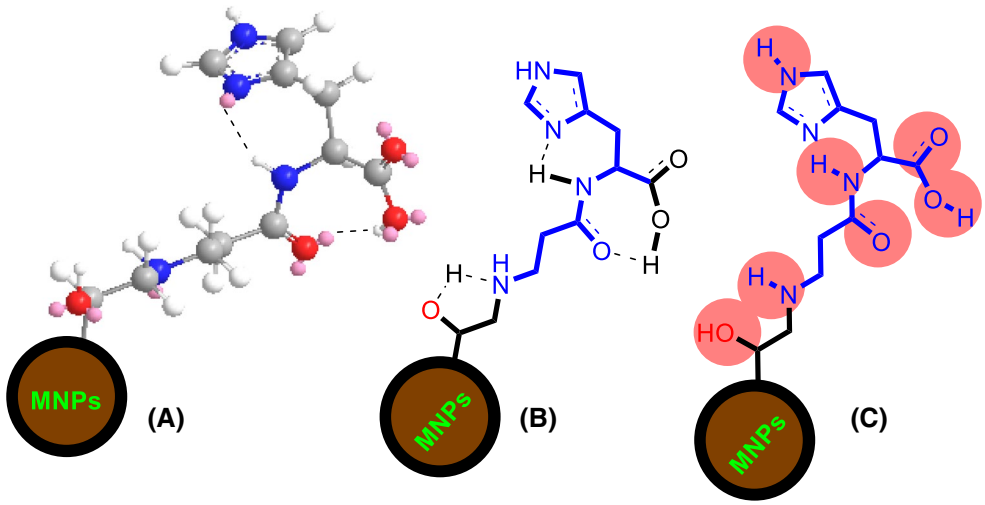

Fig. 4 The chemical structures of L-CarMNP catalyst and its catalytic sites

The catalytic activity of L-CarMNP was tested for synthesis of diverse xanthene and acridine derivatives under optimized conditions (Table 2).

As given in Table 2, by selection of different amines and aldehyde it is possible to synthesize diverse derivatives of this class of acridine and xanthene in good to excellent yields by using L-CarMNP catalyst. Both amines and aldehyde with electron-donating and electron-withdrawing groups were used, and all of the products were obtained in high yields. Also, the reusability of L-CarMNP was checked in model reaction (synthesis of **4a**) under optimized reaction conditions (Table 1, entry 5), and it was reusable at least for eight times without significant decreasing in its catalytic activity (Fig. 3).

What is important here is that which functionality in the structure of L-CarMNP catalyst system is engaged in the activation of organic components to undergo in the reaction. The catalytic activity action of amino acids is essentially originated from amino and carboxylic acid groups [59, 60]. Carboxylic acid group can protonate functionalities in molecule that can abstract hydrogen, resulting in the activation of molecule [61]. The amino group has nucleophilicity power and can help in the activation of molecules via iminium formation and Michael addition [62]. It should be mentioned that both amino and carboxylic acid groups can activate molecules through hydrogen bonding [63]. Other functional groups in the structure of amino acid may participate in the activation of molecule in parallel with amino acid group. By the use of peptides as catalyst, in addition to the mentioned functions associated with amino acids the hydrogen bonding of amid bonds is very important factor in the activation of molecules [64]. Also, peptides can act as enzymes and participate in the activation of molecules by interaction of organic groups and also structure folding [65].

The optimized structure of organic part of L-CarMNP shows that there are possibilities of two internal hydrogen bonding interactions in this molecule (Fig. 4) [66].

It is obvious that the functional groups of L-CarMNP that are peptide bonds, carboxylic group, imidazole ring, amino and hydroxy groups underwent in catalytic induction of molecules in order to participate in reaction. These functionalities can engage in the activation of molecule together and have synergetic effect in accomplishment of a reaction same as enzymes in biosystems [64]. The L-CarMNP catalyst has several hydrogen bond donor sites and can catalyze these MCRs using hydrogen bonding catalysis. The hydrogen bonding catalysis activity of L-CarMNP can be confirmed by deactivation test using urea [67]. Interestingly, addition of some urea (equal to mol % of catalyst) in the reaction mixture completely stops the reaction progress, demonstrating that the peptide nature of the catalyst and hydrogen bonding of L-CarMNP is important in its catalytic activity.

Conclusions

In summary, L-carnosine was grafted to magnetic nanoparticle surface chemically using an efficient synthetic approach, and it was used as a new nano-organocatalyst for reaction in water media at room temperatures. The catalytic activity of L-CarMNP was compared with some other catalyst systems, and results demonstrate that it has high activity in aqueous reaction media at room temperature in comparison with others. The catalyst was synthesized according to a well-defined reaction pathway using functionalization of magnetic nanoparticle surface via oxiran chemistry. Also, L-CarMNP is a magnetic reusable

organocatalyst which can be separated from the reaction mixture using an external magnetic field and has high potential to be used in other organic transformations in future.

Experimental section

General

Chemicals were purchased from Fluka and Aldrich Chemical Companies and used without further purification. ^{1}H and ^{13}C NMR spectra were recorded on a Bruker Avance 250 MHz spectrometer in DMSO-d_6 or $CDCl_3$ solution with TMS as an internal standard. FTIR spectroscopy (Shimadzu FTIR 8300 spectrophotometer) was employed for the characterization of the compounds. Melting points were determined in open capillary tubes in a Barnstead Electrothermal 9100 BZ circulating oil melting point apparatus. The reaction monitoring was accomplished by TLC on silica gel PolyGram SILG/UV254 plates. X-ray diffraction (XRD, D8, Advance, Bruker, axs) was employed for characterization of the L-CarMNP catalyst. The scanning electron micrograph (SEM) for the L-CarMNP catalyst was obtained by SEM instrumentation (SEM, XL-30 FEG SEM, Philips, at 20 kV).

Procedure for synthesis of L-carnosine-modified magnetic nanoparticles (L-carnosine MNPS)

Preparation of Fe_3O_4 nanoparticles

Magnetic nanoparticles were prepared via co-precipitation of Fe(III) and Fe(II) ions in the presence of sodium hydroxide. In a canonical flask, a mixture of $FeCl_2.2H_2O$ (16 mmol, 2.6 g) and $FeCl_3.6H_2O$ (30 mmol, 8.1 g) was dissolved in 100 mL of deionized water. Then, the pH of this solution was increased to 11 by adding a 3 M solution of NaOH as dropwise (in a period of 5 min) at 40 °C. Subsequently, the temperature of mixture was enhanced to 80 °C and the solution was stirred for 20 min in this temperature. The magnetic nanoparticles as a dark solid were isolated from the solution by magnetic separation and washed with deionized water until pH 7 reached.

Preparation of Fe_3O_4@SiO_2 nanoparticles

Fe_3O_4@SiO_2 nanoparticles were prepared based on the literature with some modification: To a mixture of 125 mL of heptanes, 25 mL of *i*-PrOH, 20 mL of PEG-300, and 10 mL of water, 2 g of Fe_3O_4 was added. Then, the mixture was stirred by mechanical stirrer under N_2 gas for 30 min. 20 mL of tetraethyl orthosilicate (TEOS) was added to the mixture next and then the solution was stirred for 12 h at 30 °C. After the specified time, 10 mL of ammonia was added and the solution was stirred continuously for another 12 h. The precipitation was washed with ethanol (3 × 10) and collected by an external magnetic field. The desired product was dried under vacuum overnight.

Synthesis of vinyl magnetic nanoparticle (VMNP)

In a three-necked flask (100 mL) containing 70 mL of dry chloroform, 5 g of Fe_3O_4@SiO_2 was charged. Then, trimethoxy(vinyl)silane (0.44 g, 3 mmol) was added to the reaction mixture dropwise over a period of 5 min at room temperature. When the addition was completed, the mixture was stirred for 12 h under reflux condition. Then, the reaction mixture was filtered and the obtained solid was dried in a vacuum at 50 °C to obtain a vinyl MNP (VMNP) substrate (5.31 g). The presence of vinyl group on the surface of MNPs was recognized using bromine test. The amount of supported vinyl groups on the surface of MNPs was determined using elemental analysis which was in good agreement with the value that estimated with an iodine test. The results showed that there are 5.6 mmol/g ethylene groups on the surface of MNPs.

Synthesis of MNP-oxiran (MNPO)

A solution of 5 g vinyl MNP (VMNP) and H_2O_2 30% (20 mL) were stirred at 50 °C for 12 h. The resulting precipitate was filtered through a Celite pad, washed with water, and dried in a vacuum to afford the MNPO substrate (5.52 g). The presence of ethylene oxide group on the silica substrate was detected by the bright pink color of the phenolphthalein (as indicator) when air passed through an aqueous solution of NaCl. The quantitative amount of oxirane groups on the substrate was identified to be 5.4 mmol/g using elemental analysis, which it showed that a remarkable amount of vinyl groups is converted to oxirane under applied conditions.

Synthesis of L-carnosine magnetic nanoparticles (L-carnosine MNPs) catalyst

For the synthesis of L-carnosine MNPs catalyst, 0.6 g of L-carnosine was added to a prepared solution containing 5 g of MNPO in 30 mL chloroform. Then, two or three drops of Et_3N were added to the reaction mixture. Subsequently, the mixture was stirred for 12 h under reflux condition. The resulting precipitate was filtered through a Celite pad, washed with water, and dried in a vacuum.

General procedure for synthesis of xanthene derivatives using L-CarMNP catalyst

A mixture of 5,5-dimethyl-cyclohexane-dione (0.308 g, 2.2 mmol) and aldehyde (1 mmol) in L-CarMNP (5 mol %) at room temperature was stirred in a round-bottomed flask for the specified time for each compound. After completion of the reaction was confirmed by TLC, the L-CarMNP catalyst was isolated from the reaction mixture using an external magnetic field. The catalyst was washed with hot ethanol (2 × 5 mL) and used for next run. The products were purified by recrystallization in ethanol.

General procedure for synthesis of acridine in the presence of L-CarMNP catalyst

In a round-bottomed flask, a mixture of aldehyde (1 mmol), dimedone (0.308 g, 2.2 mmol), amine (1 mmol), and L-CarMNP (5 mol %) was stirred at room temperature for the specified time for each compound. When the reaction was completed (confirmed by TLC), the catalyst was separated using an external magnetic field and it was washed with hot ethanol (2 × 5 mL). The separated solid after filtration was recrystallized in ethanol to obtain pure product.

Spectral data of synthesized compounds

*10-(4-Fluorophenyl)-3,3,6,6-tetramethyl-9-(3-nitrophenyl)-3,4,6,7,9,10-hexahydroacridine-1,8(2H,5H)-dione (**4a**)*

Yield: 89% (4.33 g), white crystals, mp 243–244 °C. IR (KBr): 2984, 2849, 2370, 1712, 1695, 1578, 1488, 1365, 1141, 1110, 837,718 cm^{-1}. ^{1}HNMR (250 MHz, $CDCl_3$/TMS): 0.97 (s, 12H), 2.16 (s, 4H), 2.20 (s, 4H), 5.35 (s, 1H), 7.26 (s, 3H), 7.42 (t, J = 7.5, 2H), 7.95–8.00 (m, 2H), 8.18 (s, 1H). ^{13}C NMR (62.5 MHz, $CDCl_3$/TMS): δ = 33.4, 37.3, 44.0, 44.2, 57.4, 61.2, 132.4, 132.9, 139.5, 140.1, 141.2, 143.0, 144.1, 145.3, 148.5, 149.8, 150.1, 150.8, 153.4, 189.7. Anal. Calcd for: $C_{29}H_{29}FN_2O_4$ (487.2): C, 71.30; H, 5.98; N, 5.73. Found: C, 71.21; H, 5.90; N, 5.64.

*9,10-Bis(4-chlorophenyl)-3,3,6,6-tetramethyl-3,4,6,7,9,10-hexahydroacridine-1,8(2H,5H)-dione (**4c**)*

Yield: (92%, 389 mg), white crystals, mp 204–205 °C. IR (KBr): 2974, 2819, 2360, 1710, 1685, 1578, 1488, 1365, 1195, 1141, 1067, 910, 837,768 cm^{-1}. ^{1}HNMR (250 MHz, $CDCl_3$/TMS): 1.10 (s, 12H), 2.21 (s, 4H), 2.46 (s, 4H), 4.7 (s, 1H), 7.18 (d, J = 2.5 Hz, 2H), 7.21 (d, J = 2.5 Hz, 2H), 7.25 (d, J = 2.5 Hz, 4H). ^{13}C NMR (62.5 MHz, $CDCl_3$/TMS): δ = 51.8, 53.6, 55.3, 60.3, 64.2, 64.9, 141.2, 143.0, 145.3, 148.5, 150.1, 153.4, 156.1, 156.3, 158.7, 162.4, 190.8. Anal. Calcd for: $C_{29}H_{29}Cl_2NO_2$: C, 70.44; H, 5.91; N, 2.83. Found: C, 70.35; H, 5.84; N, 2.78.

*10-(4-Methoxyphenyl)-3,3,6,6-tetramethyl-9-(4-nitrophenyl)-3,4,6,7,9,10-hexahydroacridine-1,8(2H,5H)-dione (**4d**)*

Yield: (94%, 470 mg), white crystals, mp 264–265 °C. IR (KBr): 2934, 2849, 2360, 1676, 1655, 1508, 1448, 1365, 1165, 1141, 1087, 1976, 887,710 cm^{-1}. ^{1}HNMR (250 MHz, $CDCl_3$/TMS): 0.67 (s, 4H), 0.86 (s, 4H), 2.47 (s, 12H), 3.83 (s, 3H), 5.09 (s, 1H), 7.10 (d, J = 10 Hz, 2H), 7.35 (d, J = 7.5 Hz, 2H), 7.54 (d, J = 10 Hz, 2H), 8.11 (d, J = 7.5 Hz, 2H). ^{13}C NMR (62.5 MHz, $CDCl_3$/TMS): δ = 29.3, 29.8, 47.1, 49.2, 58.0, 61.8, 71.4, 136.4, 140.5, 144.0, 149.4, 150.4, 151.0, 152.9, 154.9, 155.7, 156.7, 190.8. Anal. Calcd for $C_{30}H_{32}N_2O_5$ (500.23); C, 71.98; H, 6.44; N, 5.60. Found: C, 71.93; H, 6.38; N, 5.55.

*9-(4-Chlorophenyl)-10-(4-methoxyphenyl)-3,3,6,6-tetramethyl-3,4,6,7,9,10-hexahydroacridine-1,8(2H,5H)-dione (**4e**)*

Yield: (92%, 450 mg), white crystals, mp 233–234 °C. IR (KBr): 2934, 2879, 2360, 1716, 1675, 1508, 1438, 1365, 1165, 1141, 1087, 1916, 897,690 cm^{-1}. ^{1}HNMR (250 MHz, $CDCl_3$/TMS): 0.94 (s, 12H), 1.80 (s, 4H), 1.87 (s, 4H), 3,91 (s, 3H), 5.22 (s, 1H), 7.2(d, J = 7.5 Hz, 2H), 7.10 (d, J = 7.5 Hz, 2H), 7.19 (d, J = 7.5 Hz, 2H), 7.34 (d, J = 7.5, 2H). ^{13}C NMR (62.5 MHz, $CDCl_3$/TMS): δ = 29.3, 29.8, 44.1, 47.1, 49.2, 53.5, 70.8, 134.8, 136.4, 139.3, 140.5, 144.0, 149.4, 150.4, 151.0, 152.9, 154.9, 188.2. Anal. Calcd for: $C_{30}H_{32}ClNO_3$ (489.2): C, 73.53; H, 6.58; N, 2.86. Found: C, 73.47; H, 6.52; N, 2.80.

*9-(4-Chlorophenyl)-10-(4-fluorophenyl)-3,3,6,6-tetramethyl-3,4,6,7,9,10-hexahydroacridine-1,8(2H,5H)-dione (**4f**)*

Yield: (90%, 429 mg), white crystals, mp 234–235 °C. IR (KBr): 2954, 2869, 2360, 1666, 1645, 1578, 1488, 1365, 1195, 1141, 1087, 1010, 887 cm^{-1}. ^{1}HNMR (250 MHz, $CDCl_3$/TMS): 1.09 (s, 12H), 2.18 (s, 4H), 2.43 (s, 4H), 4.69 (s, 1H), 7.19 (s, 4H), 7.23 (s, 4H). ^{13}C NMR (62.5 MHz, $CDCl_3$/TMS): δ = 44.4, 44.8, 47.5, 50.5, 57.7, 62.3, 130.1, 131.4, 131.7, 134.3, 137.3, 139.4, 143.5, 145.1, 147.1, 162.0, 191.8. Anal. Calcd for $C_{29}H_{29}ClFNO_2$ (477.19): C, 72.87; H, 6.12; N, 2.93. Found: C, 72.79; H, 6.03; N, 5.84.

*10-(4-Fluorophenyl)-3,3,6,6-tetramethyl-9-(4-nitrophenyl)-3,4,6,7,9,10-hexahydroanthracene-1,8(2H,5H)-dione (**4g**)*

Yield: (91%, 443 mg), white crystals, mp 233–234 °C. IR (KBr): 2954, 2829, 2370, 1715, 1695, 1578, 1488, 1365, 1195, 1141, 1110, 837, 758 cm^{-1}. ^{1}HNMR (250 MHz, $CDCl_3$/TMS): 1.12 (s, 12H), 1.55 (s, 4H), 2.49 (s, 4H), 4.82 (s, 1H), 7.24 (d, J = 7.5 Hz, 4H), 7.46 (d, J = 7.5 Hz, 2H), 8.09 (d, J = 7.5 Hz, 2H). ^{13}C NMR (62.5 MHz, $CDCl_3$/TMS): δ = 33.4, 37.3, 39.0, 51.8, 58.2, 60.3, 132.4, 139.5, 140.1, 143.0, 145.3, 145.8, 149.8, 153.4, 154.7, 156.1, 191.9. Anal. Calcd for: $C_{30}H_{30}FNO_4$ (487.2): C, 73.90; H, 6.20; N, 2.87. Found: C, 73.82; H, 6.14; N, 2.81.

*9-(4-Hydroxyphenyl)-10-(4-methoxyphenyl)-3,3,6,6-tetramethyl-3,4,6,7,9,10-hexahydroacridine-1,8(2H,5H)-dione (**4h**)*

Yield: (89%, 434 mg), white crystals, mp 265–266 °C. IR (KBr): 2974, 2859, 2390, 1692, 1655, 1538, 1468, 1315, 1141, 1110, 827,699 cm^{-1}. ^{1}HNMR (250 MHz, $CDCl_3$/TMS): 0.95 (s, 4H), 1.56 (s, 12H), 2.15 (s, 4H), 3.92 (s, 3H), 5.20 (s, 1H), 6.66 (d, J = 7.5 Hz, 2H), 7.05 (s, 2H), 7.11 (s, 2H), 7.26 (s, 2H). ^{13}C NMR (62.5 MHz, $CDCl_3$/TMS): δ = 33.5, 34.7, 47.5, 52.9, 57.7, 60.9, 62.3, 139.4, 141.7, 145.1, 145.9, 146.2, 147.7, 147.9, 148.7, 150.4, 150.9, 190.5. Anal. Calcd for: $C_{30}H_{33}NO_4$ (487.22): C, 76.41; H, 7.05; N, 2.97. Found: C, 76.35; H, 6.98; N, 2.91.

*3,3,6,6-Tetramethyl-9-(4-nitrophenyl)-3,4,5,6,7,9-hexahydro-1H-xanthene-1,8(2H)-dione (**4i**)*

Yield: (90%, 356 mg), white crystals, mp 234–235 °C. IR (KBr): ν = 2954, 2869, 2360, 1666, 1620, 1512, 1465, 1365, 1203, 1141, 1002, 864, 833, 740, 694 cm^{-1}. ^{1}H NMR (250 MHz, $CDCl_3$/TMS): 1.11 (s, 12H), 2.20 (s, 4H), 2.49 (s, 4H), 4.82 (s, 1H), 7.46 (d, J = 10 Hz, 2H), 8.08 (d, J = 7.5, 2H). ^{13}C NMR (62.5 MHz, $CDCl_3$/TMS): δ = 19.7, 29.2, 37.2, 37.7, 40.1, 40.8 122.3, 123.4, 129.3, 134.3, 153.9, 162.9, 184.7. Anal. Calcd for $C_{23}H_{25}NO_5$ (395.17): C, 69.86; H, 6.37; N, 3.54. Found: C, 69.80; H, 6.31; N, 3.47.

*9-(4-Chlorophenyl)-3,3,6,6-tetramethyl-3,4,5,6,7,9-hexahydro-1H-xanthene-1,8(2H)-dione (**4j**)*

Yield: (92%, 353 mg), white crystals, mp 205–206 °C. IR (KBr): ν = 2962, 2869, 2360, 1666, 1640, 1357, 1296, 1196, 1164, 1087, 1002, 848, 717, 671 cm^{-1}. ^{1}H NMR (250 MHz, $CDCl_3$/TMS): 1.10 (s, 12H), 2.20 (s, 4H), 2.46 (s, 4H), 4.69 (s, 1H), 7.18- 7.24 (m, 4H). ^{13}C NMR (62.5 MHz, $CDCl_3$/TMS): δ = 29.2, 36.4, 40.8, 46.2, 50.7, 55.6, 130.2, 141.7, 150.6, 152.0, 157.0, 162.2. 189.7. Anal. Calcd for $C_{23}H_{25}ClO_3$ (384.15): C, 71.77; H, 6.55. Found: C, 71.70; H, 6.48.

*9-(3-Chlorophenyl)-3,3,6,6-tetramethyl-3,4,5,6,7,9-hexahydro-1H-xanthene-1,8(2H)-dione (**4k**)*

Yield: (88%, 338 mg), white crystals, mp 202–203 °C. IR (KBr): ν = 2954, 2869, 2314, 1720, 1604, 1473, 1419, 1380, 1288, 1226, 1141, 1072, 987, 948, 856, 748, 694, 655 cm^{-1}. ^{1}H NMR (250 MHz, $CDCl_3$/TMS): 1.10 (s, 12H), 2.17 (s, 4H), 2.40 (s, 4H), 5.62 (s, 1H), 7.14–7.21 (m, 1H), 7.26 (s, 1H), 7.37 (d, J = 7.5 Hz, 2H). ^{13}C NMR (62.5 MHz, $CDCl_3$/TMS): δ = 32.0, 32.1, 40.5, 42.2, 44.7, 45.8, 126.4, 126.8, 127.6, 129.3, 130.3, 142.3, 154.2, 158.8, 189.7. Anal. Calcd for $C_{23}H_{25}ClO_3$(384.15): C, 71.77; H, 6.55; Cl, 9.21; O, 12.47.

*9-(4-Fluorophenyl)-3,3,6,6-tetramethyl-3,4,5,6,7,9-hexahydro-1H-xanthene-1,8(2H)-dione (**4l**)*

Yield: 90% (3.31 g), white crystals, mp 234–235 °C. IR (KBr): 2956, 2849, 2324, 1660, 1603, 1419, 1300, 1208, 1141, 1072, 987, 856, 748, 699, 645 cm^{-1}. ^{1}H NMR (250 MHz, $CDCl_3$/TMS): 1.10 (s, 12H), 2.21 (s, 4H), 2.46 (s, 4H), 4.72 (s, 1H), 6.86–6.93 (m, 2H), 7.26 (d, J = 2.5 Hz, 2H). ^{13}C NMR (62.5 MHz, $CDCl_3$/TMS): δ = 32.2, 32.3, 40.1, 40.8, 44.9, 50.5, 114.5, 123.4, 129.3, 134.3, 162.9, 164.4, 190.3. Anal. Calcd for $C_{23}H_{25}FO_3$ (368.18): C, 74.98; H, 6.84. Found: C, 74.91; H, 6.75.

*9-(4-Hydroxyphenyl)-3,3,6,6-tetramethyl-3,4,5,6,7,9-hexahydro-1H-xanthene-1,8(2H)-dione (**4m**)*

Yield: (85%, 311 mg), white crystals, mp 259–260 °C. IR (KBr): 3409, 2869, 2823, 2715, 2360, 1651, 1612, 1521, 1450, 1357, 1203, 1002, 840, 609 cm^{-1}. ^{1}H NMR (250 MHz, $CDCl_3$/TMS): 1.09 (s, 12H)**,** 2.21 (s, 4H), 2.45 (s, 4H), 4.67 (s, 1H), 6.59 (d, J = 10 Hz, 2H), 7.10 (d, J = 10 Hz, 2H). ^{13}C NMR (62.5 MHz, $CDCl_3$/TMS): δ = 30.9, 32.2, 40.8, 44.8, 53.9, 62.6, 124.1, 125.6, 128.2, 129.4, 140.4, 149.3, 191.9. Anal. Calcd for $C_{23}H_{26}O_4$ (366.18): C, 75.38; H, 7.15. Found: C, 75.33; H, 7.08.

*3,3,6,6-Tetramethyl-9-(p-tolyl)-3,4,5,6,7,9-hexahydro-1H-xanthene-1,8(2H)-dione (**4n**)*

Yield: (87%, 320 mg), white crystals, mp 189–190 °C. IR (KBr): 2859, 2833, 2360, 1656, 1634, 1526, 1450, 1357,

1273, 1002, 840, 740. ^{1}H NMR (250 MHz, $CDCl_3$/TMS): 1.09 (s, 12H), 2.20 (s, 4H), 2.23 (s, 2H), 2.43 (s, 3H), 4.7 (s, 1H), 6.99 (d, $J = 7.5$ Hz, 2H), 7.16 (d, $J = 7.5$ Hz, 2H). ^{13}C NMR (62.5 MHz, $CDCl_3$/TMS): $\delta = 27.3$, 29.2, 32.1, 36.4, 40.8, 46.2, 47.0, 124.3, 128.2, 128.7, 129.1, 130.2, 137.0, 191.7. Anal. Calcd for $C_{24}H_{28}O_3$ (368.18): C, 79.09; H, 7.74. Found: C, 79.00; H, 7.68.

Acknowledgements Financial support from the research councils of Shiraz University is gratefully acknowledged.

References

1. D.W.C. MacMillan, Nature **455**, 304 (2008)
2. B. List, Chem. Rev. **107**, 5413 (2007)
3. J. Alemán, S. Cabrera, Chem. Soc. Rev. **42**, 774–793 (2013)
4. A.G. Doyle, E.N. Jacobsen, Chem. Rev. **107**, 5713 (2007)
5. B. Simmons, A.M. Walji, D.W.C. MacMillan, Angew. Chem. Int. Ed. **48**, 4349 (2009)
6. N.D. Shapiro, V. Rauniyar, G.L. Hamilton, J. Wu, F.D. Toste, Nature **470**, 245 (2011)
7. M. Uyanik, H. Okamoto, T. Yasui, K. Ishihara, Science **328**, 1376 (2010)
8. P. Kwiatkowski, T.D. Beeson, J.C. Conrad, D.W.C. MacMillan, J. Am. Chem. Soc. **133**, 1738 (2011)
9. F. Zhou, H. Yamamoto, Org. Lett. **18**, 4974 (2016)
10. T. Wang, X. Han, F. Zhong, W. Yao, Y. Lu, Acc. Chem. Res. **49**, 1369 (2016)
11. J. Li, S. Luo, J.P. Cheng, J. Org. Chem. **74**, 1747 (2009)
12. L.W. Xu, Y. Lu, Org. Biomol. Chem. **6**, 2047 (2008)
13. F. Zhong, X. Han, Y. Wang, Y. Lu, Chem. Sci. **3**, 1231 (2012)
14. Z. Chai, G. Zhao, Catal. Sci. Technol. **2**, 29 (2012)
15. J. Paradowska, M. Stodulski, J. Mlynarski, Angew. Chem. Int. Ed. **48**, 4288 (2009)
16. E.R. Jarvo, S.J. Miller, Tetrahedron **58**, 2481 (2002)
17. Y. Qiao, A.D. Headley, Catalysts **3**, 709 (2013)
18. Y. Huangfu, Q. Sun, S. Pan, X. Meng, F.-S. Xiao, ACS Catal. **5**, 1556 (2015)
19. A.C. Evans, A. Lu, C. Ondeck, D.A. Longbottom, R.K. O'Reilly, Macromolecules **43**, 6374 (2010)
20. M. Heidlindemann, G. Rulli, A. Berkessel, W. Hummel, H. Gröger, ACS Catal. **4**, 1099 (2014)
21. S. Calogero, D. Lanari, M. Orrù, O. Piermatti, F. Pizzo, L. Vaccaro, J. Catal. **277**, 112 (2011)
22. I. Atodiresei, C. Vila, M. Rueping, ACS Catal. **5**, 1972 (2015)
23. J. Guan, B. Liu, X. Yang, J. Hu, C. Wang, Q. Kan, ACS Sustain. Chem. Eng. **2**, 925 (2014)
24. C. Ayats, H.A. Henseler, E. Dibello, M.A. Pericàs, ACS Catal. **4**, 3027 (2014)
25. J. Mlynarski, J. Paradowska, Chem. Soc. Rev. **37**, 1502 (2008)
26. J. Mlynarski, S. Baś, Chem. Soc. Rev. **43**, 577 (2014)
27. P.R. Davies, Top. Catal. **59**, 671 (2016)
28. P. Howlader, P. Das, E. Zangrando, P.S. Mukherjee, J. Am. Chem. Soc. **138**, 1668 (2016)
29. B.I. Kharisov, H.V.R. Dias, O.V. Kharissova, A. Vazquez, Y. Pena, I. Gomez, RSC Adv. **4**, 45354 (2014)
30. M.B. Gawande, P.S. Branco, R.S. Varma, Chem. Soc. Rev. **42**, 3371 (2013)
31. M.B. Gawande, R. Luque, R. Zboril, ChemCatChem **6**, 3312 (2014)
32. M.B. Gawande, Y. Monga, R.K. Sharma, Coord. Chem. Rev. **288**, 118 (2015)
33. R.K. Sharma, S. Dutta, S. Sharma, R. Zboril, R.S. Varma, M.B. Gawande, Green Chem. **18**, 3184 (2016)
34. D. Wang, D. Astruc, Chem. Rev. **114**, 6949 (2014)
35. M.I. Majeed, Q. Lu, W. Yan, Z. Li, I. Hussain, M.N. Tahir, W. Tremel, B. Tan, J. Mater. Chem. B **1**, 2874 (2013)
36. A. Zablotskaya, I. Segal, E. Lukevics, M. Maiorov, D. Zablotsky, E. Blums, I. Shestakova, I. Domracheva, J. Mag. Mag. Mater. **321**, 1428 (2009)
37. M.B. Gawande, A. Velhinho, I.D. Nogueira, C.A.A. Ghumman, O.M.N.D. Teodorod, P.S. Branco, RSC Adv. **2**, 6144 (2012)
38. P. Riente, C. Mendoza, M.A. Pericás, J. Mater. Chem. **21**, 7350 (2011)
39. V. Polshettiwar, B. Baruwati, R.S. Varma, Chem. Commun. **14**, 1837 (2009)
40. A. Khalafi-Nezhad, M. Nourisefat, F. Panahi, RSC Adv. **4**, 22497 (2014)
41. A. Khalafi-Nezhad, M. Nourisefat, F. Panahi, Org. Biomol. Chem. **13**, 7772 (2015)
42. F. Panahi, S. Khajeh Dangolani, A. Khalafi-Nezhad, ChemistrySelect **1**, 3541 (2016)
43. A. Khalafi-Nezhad, F. Panahi, R. Yousefi, S. Sarrafi, Y. Gholamalipour, J. Iran. Chem. Soc. **11**, 1311 (2014)
44. M. Nourisefat, F. Panahi, M. Nabipour, S. Heidari, A. Khalafi-Nezhad, J. Iran. Chem. Soc. **13**, 1853 (2016)
45. Z. Durmusa, H. Kavas, A. Baykal, H. Sozeri, L. Alpsoy, S.Ü. Çelik, M.S. Toprak, J. Alloys Compd. **509**, 2555 (2011)
46. R.I. Kureshy, S. Singh, N.H. Khan, S.H.R. Abdi, E. Suresh, R.V. Jasra, J. Mol. Catal. A Chem. **264**, 162 (2007)
47. M.L. Branham, P. Singh, K. Bisetty, M. Sabela, T. Govender, Molecules **16**, 10269 (2011)
48. C. Wang, H. Daimon, S. Sun, Nano Lett. **9**, 1493 (2009)
49. R.P. Gore, A.P. Rajput, Drug Invent. Today **5**, 148 (2013)
50. M. Haji, Beilstein J. Org. Chem. **12**, 1269 (2016)
51. J.E. Biggs-Houck, A. Younai, J.T. Shaw, Curr. Opin. Chem. Biol. **14**, 731 (2010)
52. E. Rogijter, R.V.A. Orru, Drug Discov. Today: Technol. **10**, 15 (2013)
53. B.H. Rotstein, S. Zaretsky, V. Rai, A.K. Yudin, Chem. Rev. **114**, 8323 (2014)
54. M.S. Singh, S. Chowdhury, RSC Adv. **2**, 4547 (2012)
55. K. Niknam, F. Panahi, D. Saberi, M. Mohagheghnejad, J Heterocycl. Chem. **47**, 292 (2010)
56. H.R. Safaei, M. Safaei, M. Shekouhy, RSC Adv. **5**, 6797 (2015)
57. F. Shirini, P.N. Moghadam, S. Moayedi, M. Seddighi, RSC Adv. **4**, 38581 (2014)
58. A. Khalafi-Nezhad, F. Panahi, S. Mohammadi, H.O. Foroughi, J. Iran. Chem. Soc. **10**, 189 (2013)
59. Q. Yang, M. Sherbahn, T. Runge, ACS Sustain. Chem. Eng. **4**, 3526 (2016)
60. K. Sakthivel, W. Notz, T. Bui, C.F. Barbas III, J. Am. Chem. Soc. **123**, 5260 (2001)
61. Z. Li, X. Li, X. Ni, J.-P. Cheng, Org. Lett. **17**, 1196 (2015)
62. B. List, Tetrahedron **58**, 5573 (2002)
63. Y. Lu, T.C. Johnstone, B.A. Arndtsen, J. Am. Chem. Soc. **131**, 11284 (2009)
64. A.E. Allen, D.W.C. MacMillan, Chem. Sci. **3**, 633 (2012)
65. G.L. Holliday, J.B.O. Mitchel, J.M. Thornton, J. Mol. Biol. **390**, 560 (2009)
66. E.M. Moustafa, I. Ritacco, E. Sicilia, N. Russo, T. Shoeib, Phys. Chem. Chem. Phys. **17**, 12673 (2015)
67. L. Gianfreda, G. Marrucci, G. Greco, Biotechnol. Bioeng. **28**, 1647 (1986)